

Article

Study on Dual Modification of Al-17%Si Alloys by Structural Heredity

Jing Zhang ^{1,*}, Hongmei Chen ², Hui Yu ³ and Yunxue Jin ²

¹ School of Metallurgy and Materials Engineering, Jiangsu University of Science and Technology, Zhangjiagang 215600, China

² School of Materials Science and Engineering, Jiangsu University of Science and Technology, Zhenjiang 212003, China; E-Mails: hmchen@just.edu.cn (H.C.); jinyunxue@126.com (Y.J.)

³ School of Materials Science and Engineering, Hebei University of Technology, Tianjin 300132, China; E-Mail: yuhuidavid@gmail.com

* Author to whom correspondence should be addressed; E-Mail: sdzhangjing@126.com; Tel.: +86-512-5673-1519; Fax: +86-512-5673-1530.

Academic Editor: Hugo F. Lopez

Received: 30 April 2015 / Accepted: 13 June 2015 / Published: 22 June 2015

Abstract: In this study, Al-17%Si alloys were dual modified by fine-grained structural materials (FSM) according to structural heredity. Microstructure and thermal analyses were undertaken to study the modification effect of the FSM master alloy on primary and eutectic Si. Primary Si is refined to a smaller size and eutectic Si is modified from needle-like to fibrous shape after FSM master alloy addition. The optimal content of FSM master alloy is 20% and the holding time is 15min. Finer FSM master alloy leads to finer Al-17%Si alloy microstructure and more area percentage of α -Al. DSC analyses results show that FSM master alloy can raise the precipitation temperatures of primary and eutectic Si, meanwhile it can reduce the latent heat of Si solidification process.

Keywords: hypereutectic Al-Si alloys; dual modification; structural heredity

1. Introduction

Hypereutectic Al-Si alloys are ideal materials for manufacturing engines, pistons and cylinders because of their small coefficient of thermal expansion, good wear resistance and casting properties [1–4]. However, bulky primary Si and needle-like eutectic Si are harmful to the mechanical properties. This is because the brittleness of coarse Si particles lead to premature cracks initiation and fracture in tension [5]. Ultimate tensile strength of A390 alloys can be enhanced from 268.3 MPa to 317.2 MPa after modifying the Si morphologies in a previous study [5]. Therefore, dual modification of primary and eutectic Si is the key for hypereutectic Al-Si alloys. P is an effective element for primary Si modification [6,7]. However, P has no modification effect on the eutectic Si. Accordingly, complex modification combining two or more chemical elements is widely studied. Ca combining P [8], Sr combining P [9,10] and Rare Earth elements combining P [11] can all achieve a complex modification effect on primary and eutectic Si for hypereutectic Al-Si alloys.

Melt processing such as overheating is another effective method to modify primary and eutectic Si [12–14]. The modification mechanism is based on the structural heredity. It has been proved that structural heredity is an objective law during solidification process [15]. It means the original structure has a great influence on the final structure because of the existing genetic factors in raw materials. The genetic factors of Al-Si alloys are unmelted Si clusters of nano size in conventional casting process [16]. In other words, the coarse structure of primary and eutectic Si can be inherited to the final Al-Si structure via the Si clusters in original melt at normal casting temperature. Thereby, melt processing for Al-Si alloys such as heated to high temperature can obtain fine structure because of eliminating the influence of the original genetic factors. However, it is inclined to result in casting defects, such as pores, in high temperature. It is known that hydrogen can dissolve easily in Al melt. In addition, the solid solubility value increases with the temperature. Therefore it is not suitable to raise the Al melt to a very high temperature to modify Si morphologies. From a different angle of structural heredity, the Al-Si alloys can also be refined in case fine-grained structural material (FSM for short) was added into the original charging at normal casting temperature [17]. It is because the genetic factors in the FSM can inherit the fine structure to final Al-Si alloys.

Accordingly, in this work the Al-17%Si alloy billets were dual modified by adding FSM of the same composition as the master alloy due to the structural heredity. The effect of this FSM master alloy on the modification effect of primary and eutectic Si was studied.

2. Experimental Section

Both of the FSM master alloys and the base alloys used in this study are binary Al-17%Si alloys. The FSM master alloys were prepared by water-cooled copper mold and melt spinning process, respectively. The casting temperature was 950 °C for water-cooled copper mold and the cooling rate is about 10² K/s. The inner diameter of the cooper mold is 30 mm. The samples were chosen from the middle part of the master alloy. Thereby, the size of primary and eutectic Si stands for the average size.

The instantaneous temperature was 1300 °C and the speed of copper roller was 40 m/s for melt spinning process. The cooling rate is almost 10⁶ K/s. The macroscopic morphology of this master alloy is thin band, 2–3 mm wide and 100 μm thick. The microstructure of FSM master alloys is shown in Figure 1.

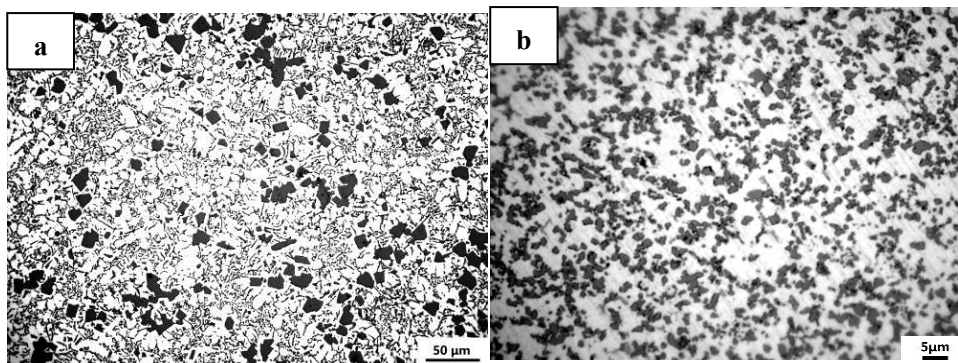


Figure 1. Microstructure of FSM master alloy: (a) prepared by water-cooler copper mold. (b) prepared by melt spinning process.

Both primary and eutectic Si can be modified using this two preparation processes. The FSM master alloy prepared by melting spinning process has finer microstructure due to faster cooling rate. The modification process using FSM master alloys is as follows: FSM master alloys were added to Al-17%Si melt at 780 °C, holding for a certain time and then poured to a metal mold. The effect of FSM addition content (0, 10%, 20%, 30%, respectively) and holding time (15 min, 35 min, 60 min, 90 min, respectively) on the microstructure of Al-17%Si alloys was studied.

JSM-6480 Scanning Electron Microscope (JEOL, Tokyo, Japan) was used to observe the three-dimensional morphologies of primary Si. The primary and eutectic Si were deep etched apart from the matrix by 10% HCl. Netzsch STA 449C Differential Scanning Calorimetry (Netzsch, Selb, Germany) was handled to study the thermal effect during the solidification. The heating and cooling rates were both 10 °C/min.

3. Results and Discussion

3.1. Modification Processes Using FSM Master Alloy

3.1.1. Effect of FSM Master Alloy Content

Figure 2 shows the microstructure of Al-17%Si alloy with different content FSM master alloy prepared by water-cooled copper mold. The holding time of FSM master alloy is 15 min and the casting temperature is 780 °C.

Bulk primary Si and long needle-like eutectic Si are typical microstructure of unmodified Al-17%Si alloy. After 10% FSM master alloy addition, primary Si size has a little decrease while the most of the eutectic Si keeps the needle-like morphologies. Increasing master alloy amount to 20%, the primary Si size decreases to 28 μm, meanwhile the eutectic Si is modified to short rod or dot shape. However, both the primary and eutectic Si become coarser when continuing to raise the amount of FSM master alloy to 30%. Therefore, the optimal amount of FSM master alloy in this study is 20%. The results reveal that the dual modification can be achieved by adding FSM master alloy into Al-17%Si alloy melt. According to Popel [15,17,18], alloy melt will show micro-stratification when it is close to its liquidus temperature. This can be seen as a metastable micro-emulsion layer or group element enrichment of suspended colloid clusters in nano size. These nanoclusters inherit fine-grained material characteristics, which can

be the source of the metal structural characteristics. As we know, the melting point of Si is 1414 °C. However, the casting temperature is 780 °C in present work. Thereby, the FSM master alloy is inclined to form micro-inhomogeneous zones which mainly consist of atomic clusters according to structural heredity theory. Si-Si nanoclusters generating from the FSM master alloy addition are the genetic factors. These nanoclusters reserve the fine-grained structure characteristic of the master alloy, and then inherit it during the sequent solidification. Therefore, the fine solidification structures are obtained with the addition of FSM master alloy. However, the microstructure of Al-17%Si alloy with 30% master alloy addition becomes coarse. The reason is that the amount of clusters participating in nucleation (at given undercooling) increases. More latent heat release leads to recalescence with less undercooling. Thereby, the efficiency of the grain refiner reduced.

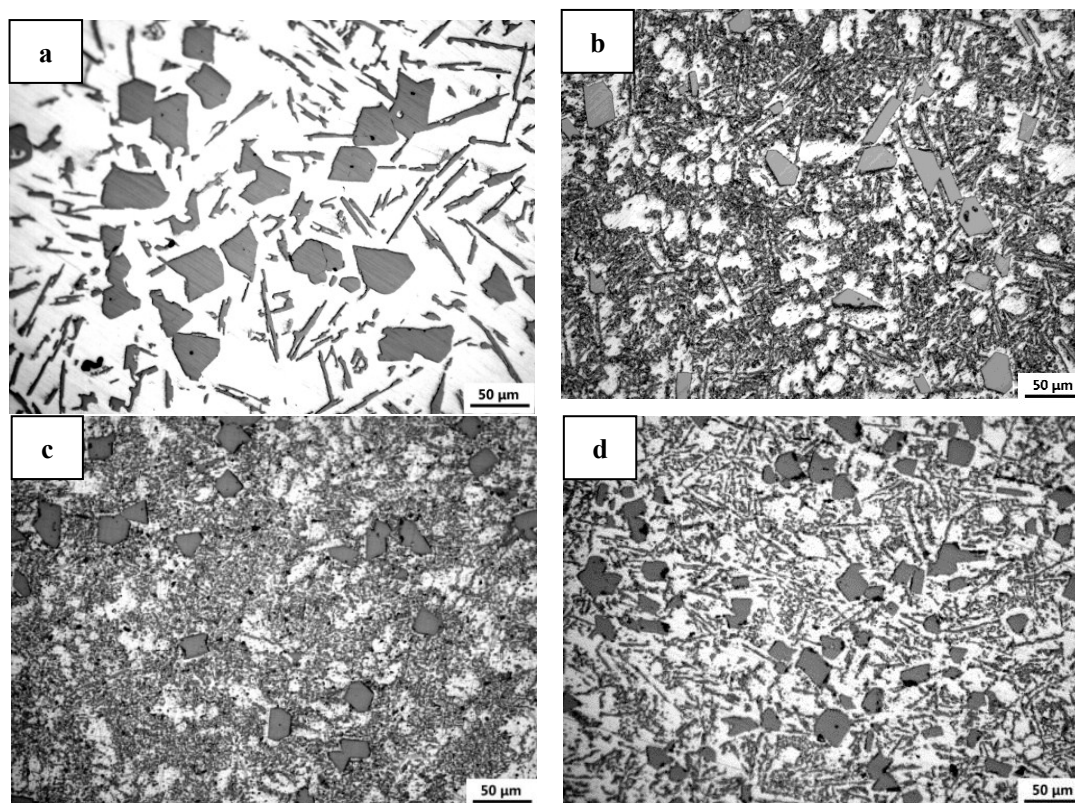


Figure 2. Microstructures of Al-17%Si alloy ingots with different content of FSM master alloys: (a) 0%; (b) 10%; (c) 20%; (d) 30%.

3.1.2. Effect of FSM master alloy holding time

The effect of FSM master alloy holding time on the modified microstructure was also studied as shown in Figure 3. The amount of FSM master alloy is 20% and casting temperature is 780 °C. Increasing holding time from 15 min to 3 min, the morphologies of primary and eutectic Si retain the same although the size of the primary Si becomes a little larger. However, star-like primary Si appears in modified Al-17%Si alloy when the holding time extends beyond 60 min in Figure 3f,h. And the primary Si size grows much larger.

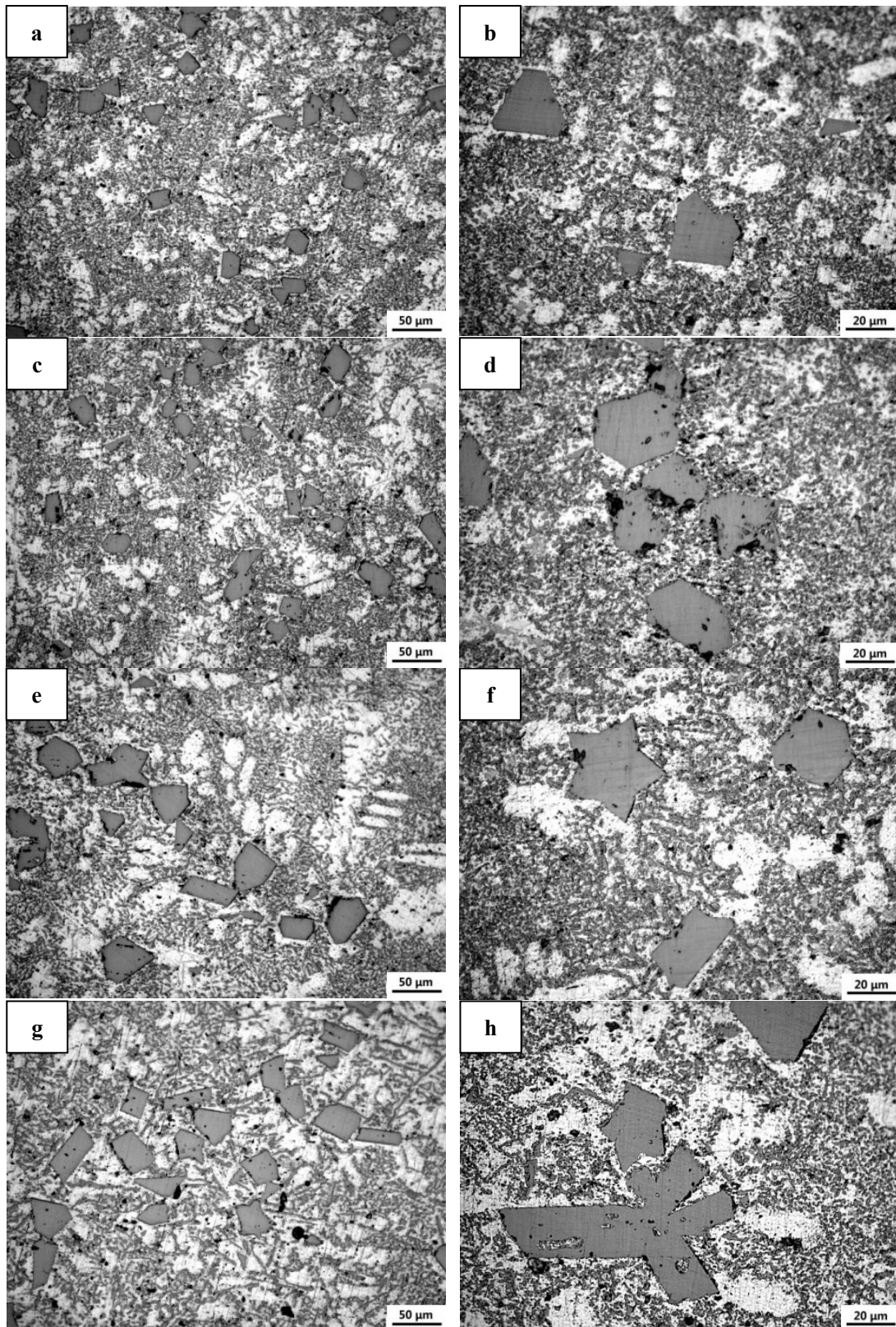


Figure 3. Microstructures of 20% FSM modified Al-17%Si alloy ingots under different holding times: (a,b) 15 min; (c,d) 35 min; (e,f) 60 min; (g,h) 95 min.

Bulk primary Si is octahedron and star-like primary Si is fivefold twinned polyhedron in three-dimensional space as shown in Figure 4. Five octahedrons can condense to one star-like primary Si because the free energy decreases spontaneously in this process. This evolving schematic has been given

by Gui as shown in Figure 5 [19]. Amounts of disperse nano Si-Si clusters appear after FSM master alloy addition. When extending the holding time, the diffusion rate of Si-Si clusters accelerates. It is much easier for the clusters gathering to form fivefold twinned crystal nucleus which result in five-star primary Si. Therefore, the optimal holding time is 15 min in present work.

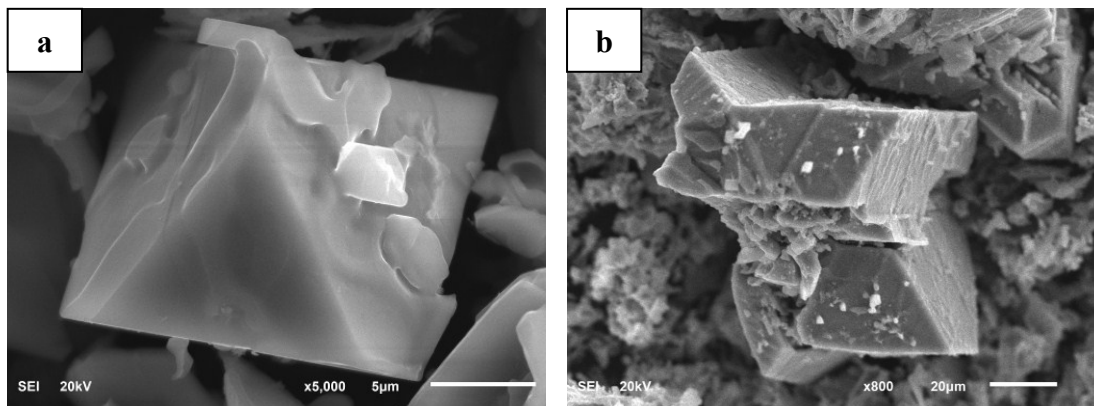


Figure 4. Different morphologies of FSM master alloy modified primary Si: (a) octahedron; (b) star-like polyhedron.

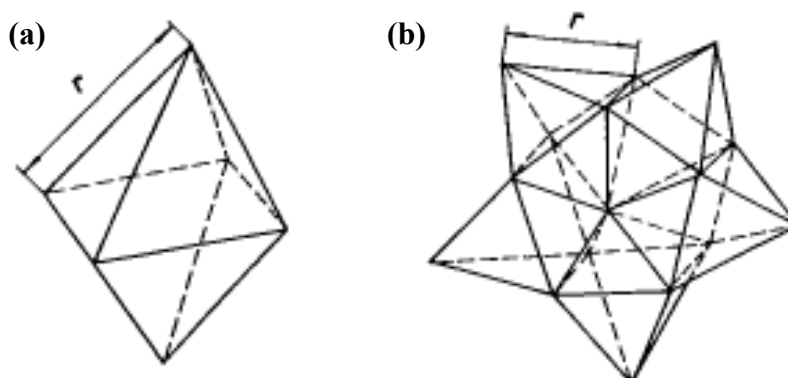


Figure 5. Schematic of different primary Si in Al-Si alloys [19]: (a) octahedron; (b) star-like polyhedron.

3.1.3. Effect of the Microstructure of FSM Master Alloy

To improve the dual modification of Al-17%Si, FSM master alloy prepared by melt spinning with finer microstructure was added into the melt. Figure 6 is the microstructure of Al-17%Si alloys with different FSM master alloys. Finer FSM master alloy results in finer modified alloy microstructure which corresponds with the structural heredity law. Primary Si size decreases to 14.3 μm and eutectic Si is completely modified. There is another characterization in Al-17%Si alloys modified by FSM master alloy. The structures of the macro-grains are evolving from (primary Si + eutectic cell) to (finer primary Si + α -Al surrounded by eutectic cell).

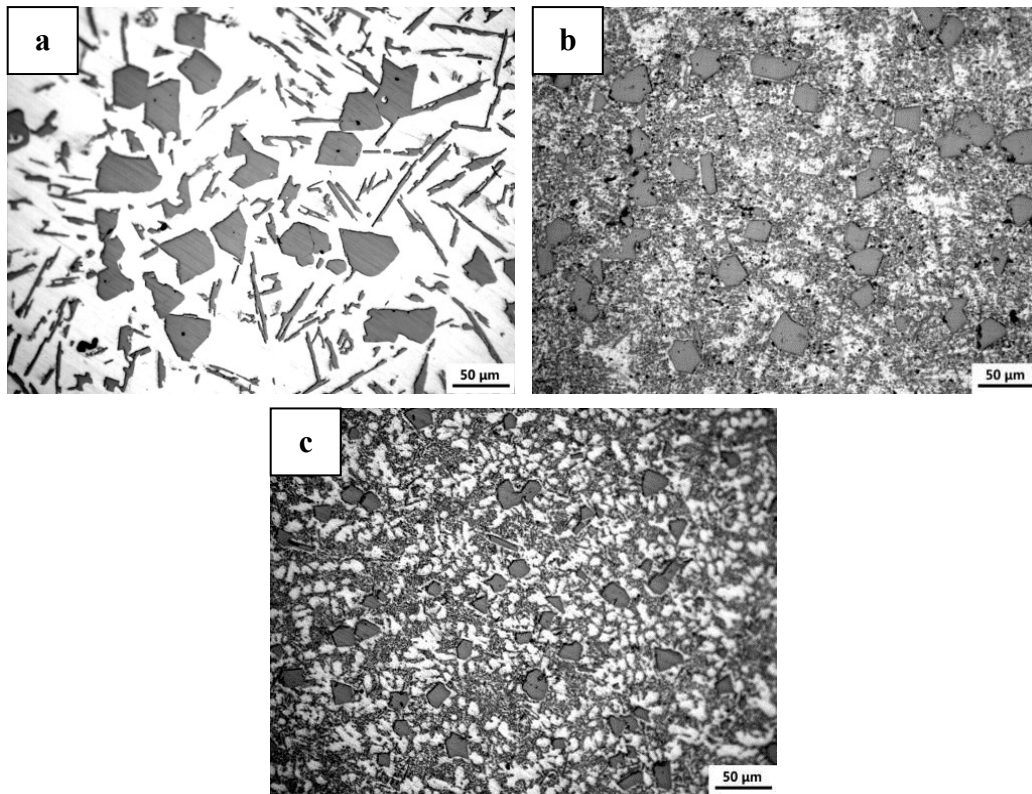


Figure 6. Microstructures of Al-17%Si alloy ingots modified by different FSM master alloy: (a) unmodified; (b) 20% FSM master alloy prepared with water-cooled copper mold; (c) 20% FSM master alloy prepared by melt spinning process.

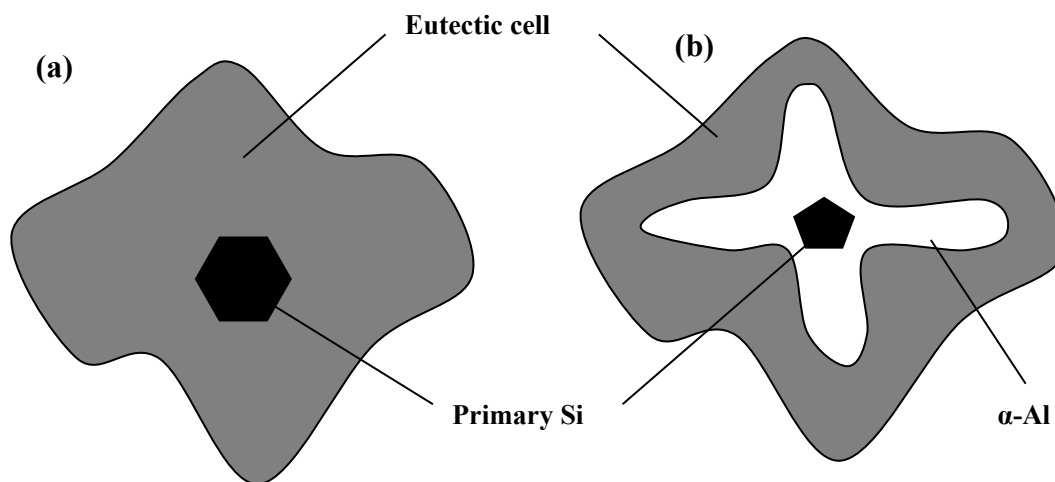


Figure 7. The structure evolving schematic of the macro-grains of Al-17%Si alloys: (a) unmodified alloys; (b) modified alloys.

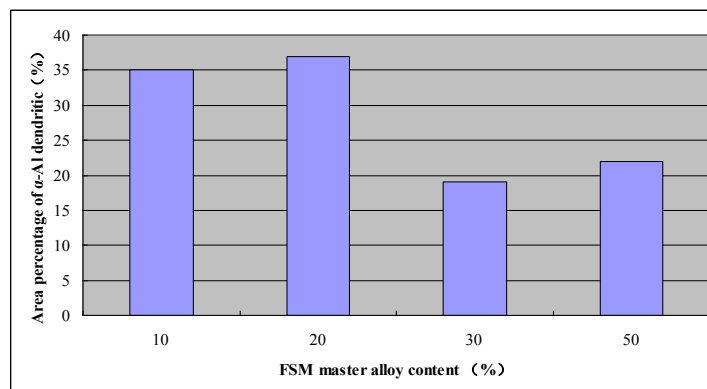


Figure 8. Effect of FSM master alloy content on the area percentage of α -Al dendrites.

The evolving schematic is shown in Figure 7. And the area of white α -Al increases when the FSM master alloy becomes finer in Figure 6c. In unmodified Al-17%Si alloy solidification process, primary Si first precipitates and then the eutectic cells crystallize when the Si content decreases to 12.6%. However, more Si-Si clusters as the nucleus appear after FSM master alloy addition, which can promote the solidification process of primary Si. This leads to Si-depleted regions around the precipitated primary Si. In other words, the components of the melt around primary Si become hypoeutectic. Finally, the macro-grain composes of three-ply structure, finer primary Si + α -Al surrounded by eutectic cell. FSM master alloy prepared by melt spinning can provide a finer crystal nucleus, which results in larger α -Al area percentage. This can also be proved by the α -Al area evolving with an increasing FSM master alloy amount in Figure 8. When the content of FSM master alloy is no more than 20%, α -Al area percentage increases. However, it decreases in amounts beyond 20%. That is because too many Si-Si clusters gather which weaken the modification effect for primary Si, which has been described in Figure 2d.

3.2. Analyses

3.2.1. SEM Analyses

Figure 9 is the 3D morphology of unmodified primary Si deep etched from Al-Si alloys.

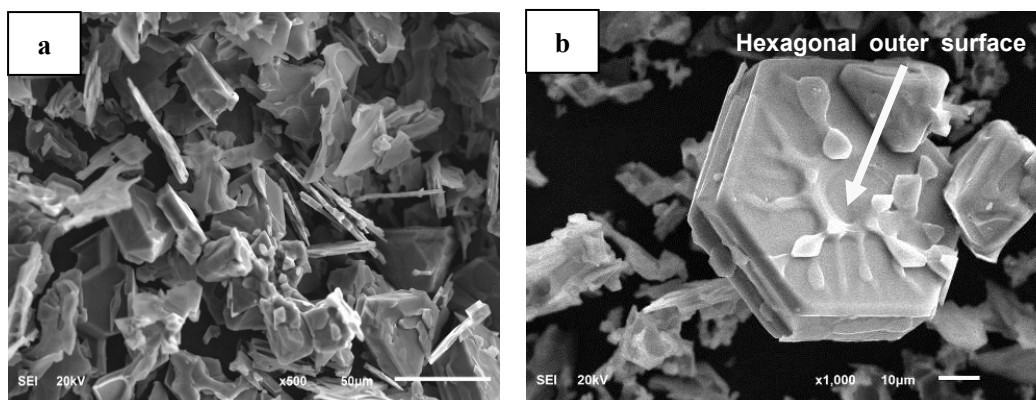


Figure 9. Morphology of primary Si in unmodified Al-17%Si alloy.

Most of the unmodified primary Si is consist of flake shape. According to Jackson's theory, Si has smooth interface in micro-scale. Jackson factor can be expressed as follows:

$$\alpha = \frac{L_0}{KT_m} \left(\frac{\eta}{\nu} \right) \quad (1)$$

In the formula, L_0 is the phase transition change of a single atom; T_m is the equilibrium crystallization temperature; η is the most adjacent number of atoms in the interface layer; ν is the coordination number. α is determined by two parts: (1) L_0/KT_m , which is dependent on the system thermodynamic properties; (2), η/ν which is named as interface orientation factor. For primary Si, $L_0/KT_m = 3.56$ [20], so

$$\alpha_{Si\{111\}} = \frac{L_0}{KT_m} \left(\frac{\eta}{\nu} \right) = 3.56 \times (3/4) = 2.76 \quad (2)$$

$$\alpha_{Si\{110\}} = \frac{L_0}{KT_m} \left(\frac{\eta}{\nu} \right) = 3.56 \times (1/4) = 0.89 \quad (3)$$

$$\alpha_{Si\{100\}} = \frac{L_0}{KT_m} \left(\frac{\eta}{\nu} \right) = 3.56 \times (2/4) = 1.78 \quad (4)$$

According to the above calculation results, the Jackson factor of $\{111\}$ primary Si crystal plane group is greater than 2, which is non-continuous facet growth pattern. Meanwhile, the Jackson factors of $\{110\}$ and $\{100\}$ primary Si crystal plane group are less than 2, which is continuous facet growth pattern. Therefore, the primary Si growth mechanism is anisotropic. And the (111) crystal face perpendicular to the slow growth of [111] crystal direction is the most densely arranged surface. The fastest growth direction is along the [112] series crystal orientation. It prefers to form 141° reentrant in the growth front, which is the TPRES (twin plane reentrant edge) mechanism of primary Si [21]. The outer surface of flake primary Si is surrounded by the densely packed (111) crystal planes. The twin re-entrant grooves sketch map of unmodified plate-like primary Si is shown in Figure 10.

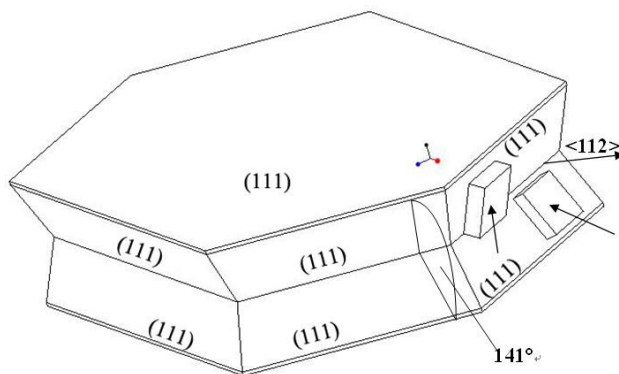


Figure 10. Twin re-entrant grooves sketch map of unmodified plate-like primary Si.

Figure 11 is the 3D morphology of modified primary Si in Al-17%Si alloys. Most of the Si shows as small octahedrons without holes or other defects. According to the research of [22], octahedral primary Si has regular angle, edge and (111) crystal planes. The intersection angle between two adjacent (111)

crystal plane is 141° . The edge growth rate $V_{\langle E \rangle}$, the angle growth rate $V_{\langle 100 \rangle}$ and the (111) crystal plane growth rate $V_{\langle 111 \rangle}$ are assumed constant. From Figure 12 [22], it can be seen that,

$$V_{\langle 111 \rangle} = V_{\langle E \rangle} \sin \alpha \tag{5}$$

$$V_{\langle E \rangle} = V_{\langle 100 \rangle} \sin \beta \tag{6}$$

$$V_{\langle 111 \rangle} = V_{\langle 100 \rangle} \sin \alpha \cdot \sin \beta \tag{7}$$

$$\frac{V_{\langle 100 \rangle}}{V_{\langle 111 \rangle}} = \frac{1}{\sin \alpha \cdot \sin \beta} = \frac{1}{\sin 70.5^\circ \cdot \sin 45^\circ} = 1.5 \tag{8}$$

Therefore, primary Si grows to perfect octahedron without defects when $V_{\langle 100 \rangle} / V_{\langle 111 \rangle} = 1.5$. In modified Al-17%Si alloys, there are no obvious holes and other defects in the surface of octahedral primary Si. It is mainly due to the FSM master alloy changing the anisotropy during the growth process of primary Si. It means the (111) crystal plane growth rate $V_{\langle 111 \rangle}$ has been increased so that the primary Si can grow to perfect octahedron.

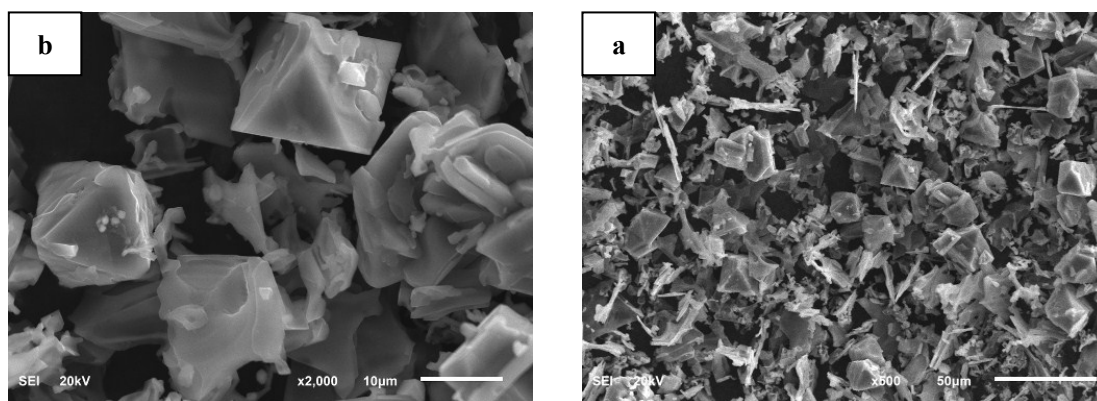


Figure 11. Morphology of primary Si in modified Al-17%Si alloy.

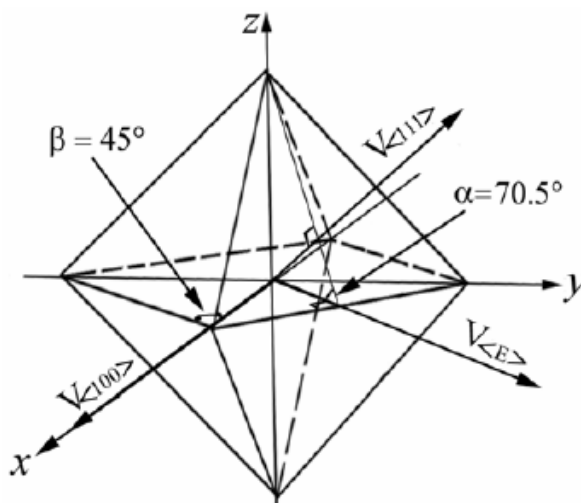


Figure 12. A schematic illustrating the vector relationship between $V_{\langle 100 \rangle}$, $V_{\langle E \rangle}$ and $V_{\langle 111 \rangle}$ [22].

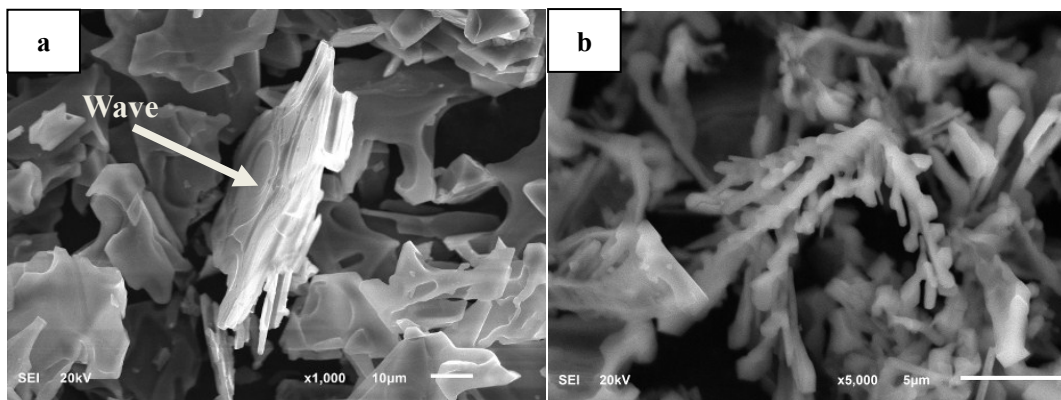


Figure 13. Morphology of eutectic Si in Al-17%Si alloy: **(a)** unmodified eutectic Si; **(b)** modified eutectic Si.

The morphologies of eutectic Si in Al-17%Si alloys convert from plate-like to coral-like shape in three-dimensions after modification, which is shown in Figure 13. The modification mechanism has been investigated in our former work [23]. The modification mechanisms can be concluded to: the Si–Si bonded nanoclusters are the genetic factors of the FSM master alloys which inherit the fine-grained structure to the HCC Al–12%Si alloy billet. On the other hand, the lattice-modulated Si clusters which have the closest structure with Si matrix will be the optimal nuclei for the eutectic Si. The mass of excess Si–Si bonded nanoclusters concentrates in the solid–liquid interface front, hindering part of the movement of the growth step in eutectic Si. Consequently, the eutectic Si modified to fine fibrous and grew via the TPPE mechanism.

3.2.2. DSC Analyses

The influence of the FSM master alloys on the thermal effect was studied by DSC analyses. Figure 14 and Table 1 are the crystallization parameters about primary Si solidification. Figure 15 and Table 2 are the crystallization parameters about eutectic Si solidification.

Primary Si precipitates in the 700–600 °C temperature range. Both the starting and peak precipitation temperatures of primary Si rise after the FSM master alloy addition. The latent heat has a little increase after 10% FSM master alloy addition prepared by water-cooled copper mold. However, there is a large decrease of latent heat after adding 10% FSM master alloy prepared by melt spinning process. Eutectic Si precipitates in the 600–500 °C temperature range. The temperature and latent heat evolving trend are as same as primary Si. Precipitation temperature raises and latent heat decreases after modification by the FSM master alloy. The latent heat of the whole Si solidification process is also calculated in Table 2. The decreasing values are 48.9 J/g for FSM master alloy addition prepared by water-cooled copper mold and 71 J/g for FSM master alloy prepared by melt spinning. In conclusion, finer FSM master alloy results in larger decreasing value of undercooling and latent heat. FSM master alloys generate plenty of Si–Si clusters which can provide more crystal nuclei for Si, the same role as AIP [5]. However, the Si–Si clusters which have more similar structure with the Si matrix can be the best heterogeneous nuclei of eutectic Si compared with other modified agents such as AIP. It is much easier to solidify in a small undercooling when there are enough external particles as the nuclei. It is an exothermic reaction for Si solidification accompanied by the combination of new Si–Si bands. FSM master alloy provides more

Si–Si clusters, which can save more energy to form new Si–Si bonds. Finer FSM master alloy can generate more small nuclei in the same holding time. Thereby, it needs less energy for Si solidification with 10% FSM master alloy prepared by melt spinning process.

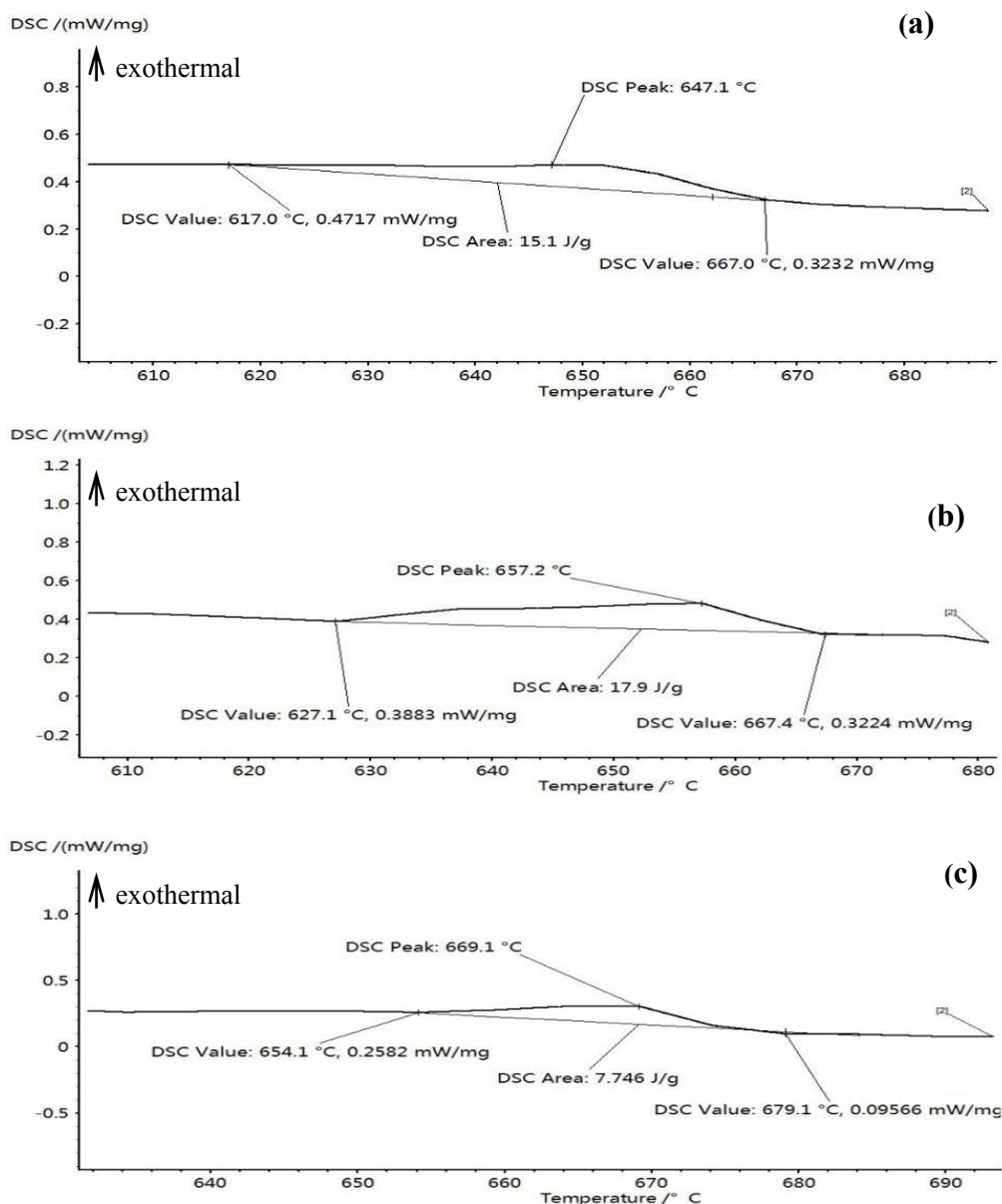


Figure 14. Part of the cooling process DSC curves between 700–600 °C: (a) unmodified alloys; (b) 10% FSM master alloy addition prepared by water-cooled copper mold; (c) 10% FSM master alloy addition prepared by melt spinning process.

Table 1. Some crystallization parameters of primary Si by DSC analyses.

Alloys	Primary Si precipitation temperature (°C)	Primary Si precipitation peak temperature (°C)	Latent heat of primary Si solidification (J/g)
a	667	647.1	15.1
b	667.4	657.2	17.9
c	679.1	669.1	7.746

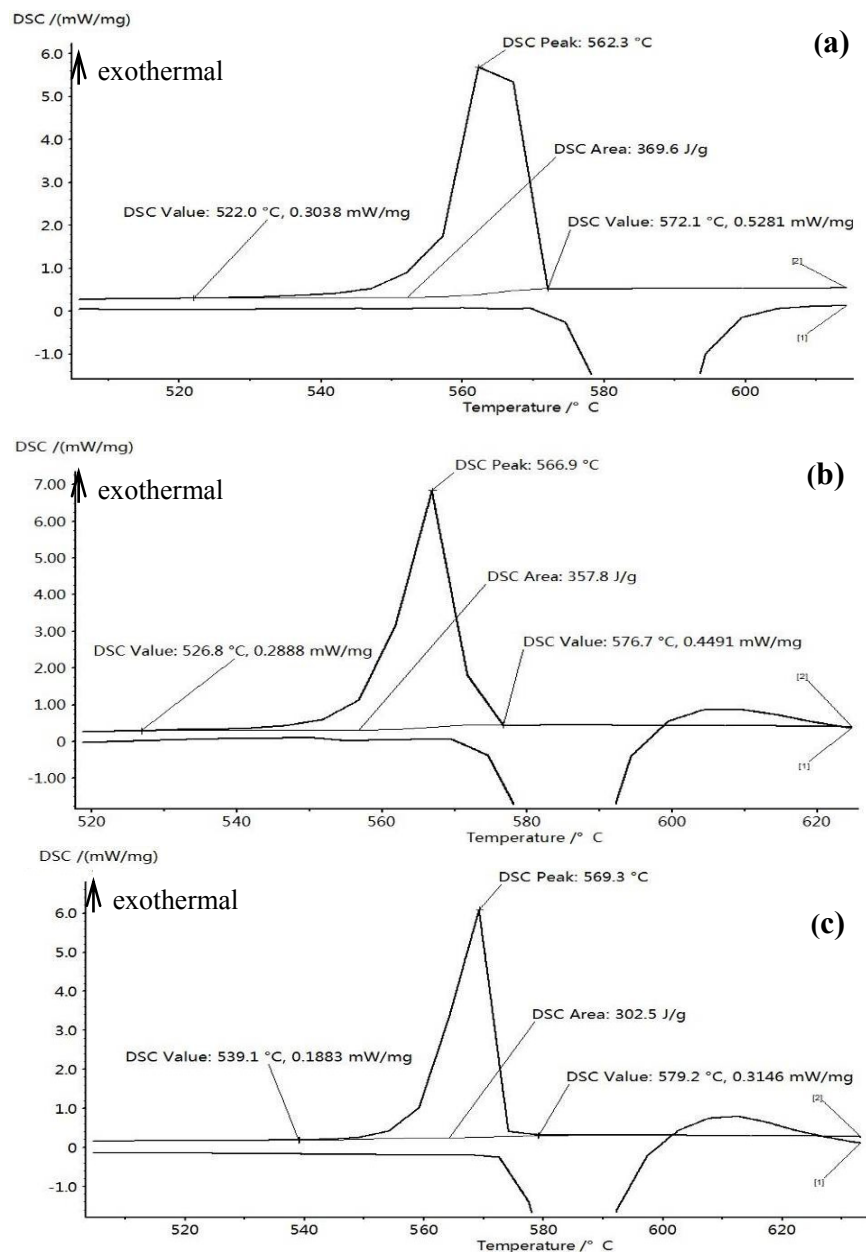


Figure 15. Part of the cooling process DSC curves between 600–500 °C: (a) unmodified alloys; (b) 10% FSM master alloy addition prepared by water-cooled copper mold; (c) 10% FSM master alloy addition prepared by melt spinning.

Table 2 Some crystallization parameters of eutectic Si by DSC analyses.

Alloys	Eutectic precipitation temperature (°C)	Eutectic precipitation peak temperature (°C)	Latent heat of eutectic solidification (J/g)	Total latent heat of Si solidification (J/g)
a	572.1	562.3	369.6	465.3
b	576.7	566.9	357.8	416.4
c	579.2	569.3	302.5	394.3

4. Conclusions

The effects of FSM master alloy on the microstructure of hypereutectic Al-17%Si alloy were investigated in this study. The following conclusions can be drawn from the results obtained.

- (1) Primary Si is refined to a smaller size and eutectic Si is modified from needle-like to fibrous shape after 20% FSM master alloy addition, which was prepared by water-cooled copper mold. The optimal content and holding time for FSM master alloy are 20% and 15 min, respectively. Increasing the content or holding time, the microstructure becomes coarser. Star-like primary Si and certain needle-like eutectic Si appear.
- (2) FSM master alloy prepared by melt spinning can lead to finer microstructure and more area percentage of α -Al in Al-17%Si compared with that fabricated by water-cooled copper mold.
- (3) The morphologies of primary Si in Al-17%Si change from big flake to octahedron shape in three-dimensions after modification. Meanwhile, the morphologies of eutectic Si convert from plate-like to coral-like shape.
- (4) DSC analyses results show that FSM master alloy can increase the precipitation temperature of primary and eutectic Si and reduce the latent heat of Si solidification process.

Acknowledgments

This research was financially supported by the National Natural Science Foundation of China (No.51201071).

Author Contributions

Jing Zhang conceived the study and wrote the paper. Hongmei Chen and Yunxue Jin performed the experiments. Hui Yu reviewed and edited the manuscript. All authors read and approved the manuscript.

Conflicts of Interest

The authors declare no conflict of interest.

References

1. Uzun, O.; Kilicaslan, M.F.; Yilmaz, F. Formation of novel flower-like silicon phases and evaluation of mechanical properties of hypereutectic melt-spun Al-20Si-5Fe alloys with addition of V. *Mater. Sci. Eng. A* **2014**, *607*, 368–375.
2. Li, P.B.; Chen, T.J.; Zhang, S.Q.; Guan, R.G. Research on semisolid microstructural evolution of 2024 aluminum alloy prepared by powder thixoforming. *Metals* **2015**, *5*, 547–564.
3. Zhao, L.Z.; Zhao, M.J.; Song, L.J.; Mazumder, J. Ultra-fine Al-Si hypereutectic alloy fabricated by direct metal deposition. *Mater. Des.* **2014**, *56*, 542–548.
4. Kilicaslan, M.F. Effect of V addition on the nano-size spherical particles growing on the Fe-bearing intermetallics and silicon phases of gas atomized hypereutectic Al-20Si-5Fe alloys. *J. Alloys Compd.* **2014**, *606*, 86–91.
5. Gao, T.; Zhu, X.Z.; Qiao, H.; Liu, X.F. A new Al-Fe-P master alloy designed for application in low pressure casting and its refinement performance on primary Si in A390 alloy at low temperature. *J. Alloys Compd.* **2014**, *607*, 11–15.

6. Liang, S.M.; Schmid-Fetzer, R. Phosphorus in Al–Si cast alloys: Thermodynamic prediction of the AlP and eutectic (Si) solidification sequence validated by microstructure and nucleation undercooling data. *Acta Mater.* **2014**, *72*, 41–56.
7. Liu, Y.; Cao, D.C.; Tu, H.; Su, X.P.; Wang, J.H.; Wu, C.J.; Peng, H.P. Phase equilibria of the Ni–Si–P system at 800 °C. *J. Alloys Compd.* **2013**, *577*, 643–649.
8. Ludwig, T.H.; Schonhovd, D.E.; Schaffer, P.L.; Arnberg, L. The effect of Ca and P interaction on the Al–Si eutectic in a hypoeutectic Al–Si alloy. *J. Alloys Compd.* **2014**, *586*, 180–190.
9. Tebib, M.; Samuel, A.M.; Ajersch, F.; Chen, X.G. Effect of P and Sr additions on the microstructure of hypereutectic Al–15Si–14Mg–4Cu alloy. *Mater. Charact.* **2014**, *89*, 112–123.
10. Zuo, M.; Zhao, D.G.; Teng, X.Y.; Geng, H.R.; Zhang, Z.S. Effect of P and Sr complex modification on Si phase in hypereutectic Al–30Si alloys. *Mater. Des.* **2013**, *47*, 857–864.
11. Wang, A.Q.; Zhang, L.J.; Xie, J.P. Effects of cerium and phosphorus on microstructures and properties of hypereutectic Al–21%Si alloy. *J. Rare Earth* **2013**, *31*, 522–525.
12. Dai, H.S.; Liu, X.F. Refinement performance and mechanism of an Al–50Si alloy. *Mater. Charact.* **2008**, *59*, 1559–1563.
13. Xu, C.L.; Jiang, Q.C. Morphologies of primary silicon in hypereutectic Al–Si alloys with melt overheating temperature and cooling rate. *Mater. Sci. Eng. A* **2006**, *437*, 451–455.
14. Li, P.J.; Nikitin, V.I.; Kandalove, E.G.; Nikintin, K.V. Effect of melt overheating, cooling and solidification rates on Al–16wt.%Si alloy structure. *Mater. Sci. Eng. A* **2002**, *332*, 371–374.
15. Bian, X.F.; Liu, X.F.; Ma, J.J. *Genetics of Cast Metals*; Shandong Science & Technology Press: Jinan, China, 1999; pp. 6–8.
16. Singh, M.; Kumar, R. Structure of liquid aluminium–silicon alloys. *J. Mater. Sci.* **1973**, *8*, 317–323.
17. Zhang, J.; Kang, S.B.; Yu, H.S.; Cho, J.H.; Min, G.H.; Stetsenko, V.Y. Effect of fine-grained raw material addition on microstructure refinement and tensile properties in horizontal continuous casting Al–12%Si alloy billets. *Mater. Des.* **2011**, *32*, 3566–3569.
18. Zhang, J.; Yu, H.S.; Kang, S.B.; Cho, J.H.; Min, G.H.; Stetsenko, V.Y. Effect of fine-grained structural Al–12%Si materials on morphologies and crystal defects of eutectic Si in HCC Al–12%Si alloy billets. *J. Alloys Compd.* **2012**, *541*, 157–162.
19. Gui, M.C.; Jia, J.; Jia, Q.C. Nucleating mechanism of five petal star-shaped primary silicon. *Acta Metal. Sinica* **1996**, *32*, 1177–1783.
20. An, G.Y. *Principle of Casting Forming*; Machinery Industry Press: Beijing, China, 1992; pp. 68–69.
21. Shamsuzzoha, M.; Hogan, L.M. The crystal morphology of fibrous silicon in strontium-modified Al–Si eutectic. *Philos. Mag. A* **1986**, *54*, 459–477.
22. Xu, C.L.; Wang, H.Y.; Liu, C.; Jiang, Q.C. Growth of octahedral primary silicon in cast hypereutectic Al–Si alloys. *J. Cryst. Growth* **2006**, *291*, 540–547.
23. Zhang, J.; Kang, S.B.; Yu, H.S.; Cho, J.H.; Min, G.H. Modification of horizontal continuous casting Al–12%Si alloy using FSM master alloy. *Mater. Charact.* **2013**, *75*, 44–50.